

## Investigation of Annealing Programs by Hot Isostatic Pressing for Crystallization of Amorphous $\text{Pb}(\text{Zr}_{0.3}\text{Ti}_{0.7})\text{O}_3$ Thin Films

Koji Fukushima, Masafumi Kobune, Yusuke Nishioka, Toru Yamaji, Tetsuo Yazawa, Hironori Fujisawa\* and Masaru Shimizu\*

Department of Materials Science and Chemistry, Graduate School of Engineering, University of Hyogo, 2167 Shosha, Himeji, Hyogo 671-2201  
Fax: +81-792-67-4897, e-mail: kobune@eng.u-hyogo.ac.jp

\*Department of Electrical Engineering and Computer Sciences, Graduate School of Engineering, University of Hyogo, 2167 Shosha, Himeji, Hyogo 671-2201

Epitaxial  $\text{Pb}(\text{Zr}_{0.3}\text{Ti}_{0.7})\text{O}_3$  films with uniform *c*-axis orientations were successfully fabricated on  $\text{PbTiO}_3/\text{Pt}(100)/\text{MgO}(100)$  substrates from an amorphous state by hot isostatic pressing (HIP) crystallization. The crystallized PZT films yielded a preferential (001) orientation with the degree of *c*-axis orientation of  $\alpha=0.68$ - $0.72$ . Based on the results of X-ray pole figures, all the PZT films fabricated using the three crystallization programs were almost completely epitaxial. From measurements of fatigue, imprint and retention characteristics, PZT films HIP-treated at 1.5 MPa using a two-step (600-700°C) annealing program have the ability to be used as high-endurance and high-density element materials for ferroelectric random access memory (FeRAM) applications.

Key words: PZT, hot isostatic pressing, FeRAM, imprint, retention

### 1. INTRODUCTION

It has been recently reported that post-annealing under pressures greater than atmospheric pressure (=0.1 MPa) is very effective for crystallizing amorphous  $\text{Pb}(\text{Zr}_x\text{Ti}_{1-x})\text{O}_3$  (PZT)<sup>1,2)</sup>,  $\text{Bi}_4\text{Ti}_3\text{O}_{12}$ <sup>3,4)</sup> and  $\text{Pb}(\text{Zn}_{1/3}\text{Nb}_{2/3})\text{O}_3$ -PZT<sup>5,6)</sup> films, as well as for improving their ferroelectric properties and memory characteristics. Epitaxial PZT films with compositions of  $\text{Pb}(\text{Zr}_x\text{Ti}_{1-x})\text{O}_3$ , where  $x=0.25$ - $0.35$ <sup>7)</sup>, have attracted significant attention recently for applications in high-density and high-reliance lead-based ferroelectric random access memories (FeRAMs) because of their large remanent polarizations ( $P_r$ ). However, thus far, there have been no studies on the ferroelectric properties and memory characteristics of  $\text{Pb}(\text{Zr}_{0.3}\text{Ti}_{0.7})\text{O}_3$  films on  $\text{PbTiO}_3$  (PT)/Pt/MgO(100) substrates that have been hot isostatic pressing (HIP)-treated by single- or multi-step annealing under pressures greater than 1.0 MPa.

In the present study, we have fabricated  $\text{Pb}(\text{Zr}_{0.3}\text{Ti}_{0.7})\text{O}_3$  films with highly uniform *c*-axis orientations on PT/Pt(100)/MgO(100) substrates from an amorphous state by hot isostatic pressing (HIP). Specifically, the crystallization of amorphous PZT films and relevant growth mechanisms are investigated using single- and multi-step annealing programs using the HIP technique. The ferroelectric properties (*P-E* measurements) and memory characteristics (fatigue, imprint and retention characteristics) of the fabricated PZT films are investigated, and the optimal annealing program for crystallization from the amorphous state is discussed.

### 2. EXPERIMENTAL

A  $\text{PbTiO}_3$  (PT) seed layer with a thickness of

30 nm was deposited on a Pt(100 nm)/MgO substrate by rf magnetron sputtering using a powder target. An amorphous PZT film was then deposited on the seed layer by rf-magnetron sputtering using a ceramic target without heating the substrate. The thickness of the PZT film after crystallization was approximately 270 nm, yielding a ferroelectric layer with a total thickness of 300 nm. The sputtering conditions for the PT seed layer, the amorphous PZT film, and the top and bottom Pt electrodes are summarized in Table 1. The as-deposited amorphous films were oxidation-treated for 10 s using a 2.2 M hydrogen peroxide solution and ultrasonic-wave vibrations, to compensate uniformly the oxygen vacancies occurred in the films and

Table 1. Sputtering conditions for fabricating  $\text{PbTiO}_3$  seed layer, amorphous PZT films, and top and bottom Pt electrodes.

Item	$\text{PbTiO}_3$ seed layer	Amorphous PZT films	Bottom Pt electrode	Top Pt electrode
Target	* $\text{PbTiO}_3$ powder	**PZT ceramic	Pt	Pt
Substrate temp. (°C)	570	R.T.	214	R.T.
Input power density ( $\text{W}/\text{cm}^2$ )	2.0	2.0	0.3	1.2
Sputtering gas ( $\text{Ar}/\text{O}_2$ )	90/10	90/10	100/0	50/50
Gas pressure (Pa)	0.8	0.4	0.4	0.5
Deposition rate (nm/min)	5.1	2.1	6.9	100

\* $\text{PbTiO}_3$  powder target;  $0.25\text{PbTiO}_3+0.75\text{PbO}$

\*\*PZT ceramic target;  $0.92\text{Pb}(\text{Zr}_{0.30}\text{Ti}_{0.70})\text{O}_3+0.08\text{PbO}$

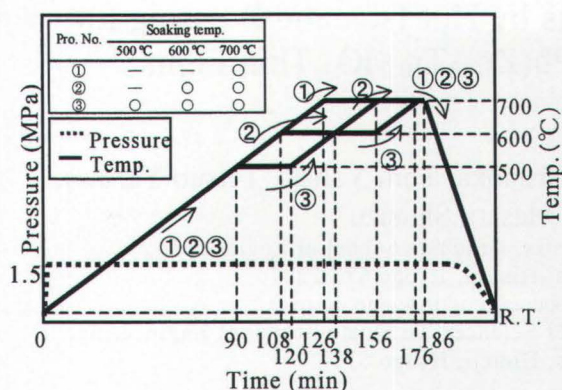


Fig. 1. Schematic diagram of single- and multi-step annealing programs with the fixed pressure condition of 1.5 MPa by HIP.

then crystallized under a mixed gas ( $Ar/O_2=80/20$ ) pressure of 1.5 MPa using HIP equipment. Three different annealing programs were employed for crystallization and these are outlined in Fig. 1. The crystalline phase, the orientation and the crystallinity of the crystallized PZT films were investigated using X-ray diffraction (XRD; RINT2200, Rigaku). The degree of  $c$ -axis orientation ( $\alpha$ ) for the tetragonal structure is defined by

$$\alpha = I(001) / \{I(001) + I(100) + I(111)\} \quad (1)$$

where  $I(001)$ ,  $I(100)$  and  $I(111)$  represent the X-ray diffraction intensities of the (001), (100) and (111) reflections. In-plane orientations of PZT/PT/Pt/MgO films were determined by XRD pole-figure measurements using a high resolution X-ray diffractometer (XRD; X'Pert-MRD, Philips). The polarization-electric field ( $P$ - $E$ ) hysteresis loops and polarization fatigue characteristics were measured using a ferroelectric film test system (RT-66A, Radiant Tech.) and a function/arbitrary waveform generator (33120A, Hewlett-Packard). Polarization fatigue tests were performed using bipolar pulses with amplitudes of 4.5-4.8 V at 500 kHz. The dc-voltage offset calculated from the measurement of the  $P$ - $E$  hysteresis loop was set so as to equalize the positive and negative fields applied to the sample. Imprint measurements were performed at room temperature using unipolar pulses with amplitudes of  $2.5E_c$  for  $2.0 \times 10^4$  s at 500 kHz to the respective positive and negative regions. Retention characteristics were investigated by preserving the samples for many hours at  $150^\circ\text{C}$  under atmospheric pressure in an electric furnace. The measurements were intermittently carried out at holding times of 10 min, 30 min, 2 h, 25 h, 100 h, 200 h, 230 h and 300 h.

### 3. RESULTS AND DISCUSSION

Figure 2 shows the XRD patterns and the degree of  $c$ -axis orientation for typical PZT films, HIP-treated using the two-step annealing program, as well as for a PZT film before HIP treatment for comparison. The crystallized PZT samples had a

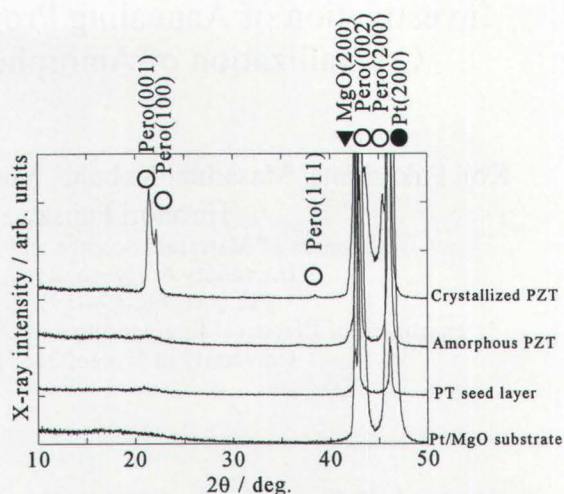


Fig. 2. XRD patterns of Pt/MgO substrate,  $PbTiO_3$  seed layer, amorphous PZT layer before HIP and typical PZT films HIP-treated by the two-step annealing program 2.

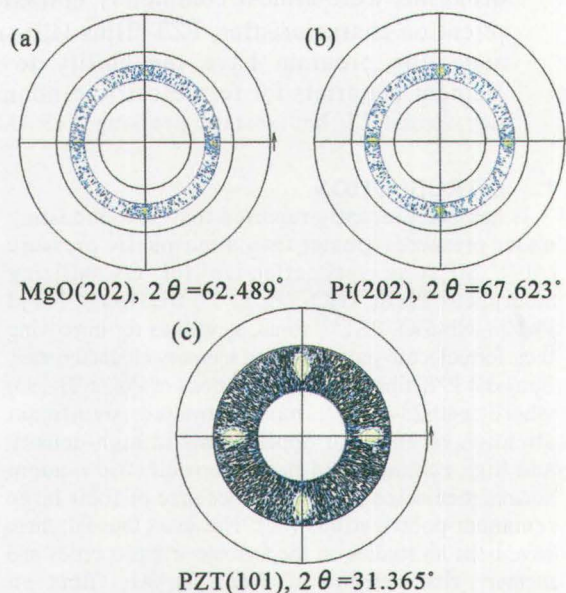


Fig. 3. XRD pole figures of PZT sample treated according to program 2 for (a)  $MgO(202)$ , (b)  $Pt(202)$  and (c)  $PZT(101)$ .

single-phase perovskite structure and strong (001) and (100) orientations if the weak (111) reflection peak was neglected. The degree of  $c$ -axis orientation of the crystallized PZT films was in the range of  $\alpha=0.68$ -0.72. The crystallinity,  $\Delta\theta$ , of the (001) reflection was in the range of  $2.3$ - $3.0^\circ$ . These results suggest that all three annealing programs adopted in this study produced good crystallization in the films. Figure 3 shows XRD pole figures of the PZT sample treated according to program 2 shown in Fig. 1, as a representative example of the three programs. Figures 3(a), 3(b) and 3(c) show XRD pole figures for  $MgO(202)$ ,  $Pt(202)$  and  $PZT(101)$ , respectively. As shown, the four-fold symmetry observed in the pole figures for

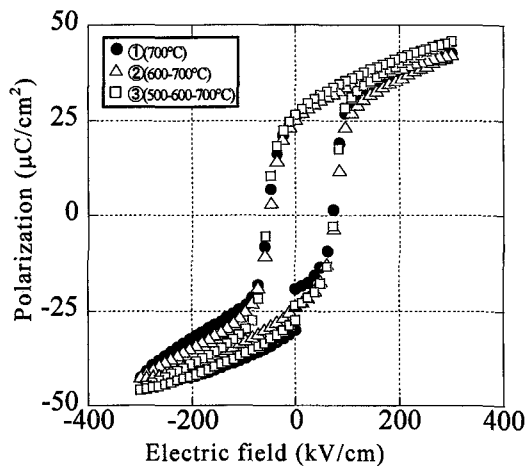


Fig. 4. *P-E* hysteresis loops of the three PZT samples crystallized by HIP.

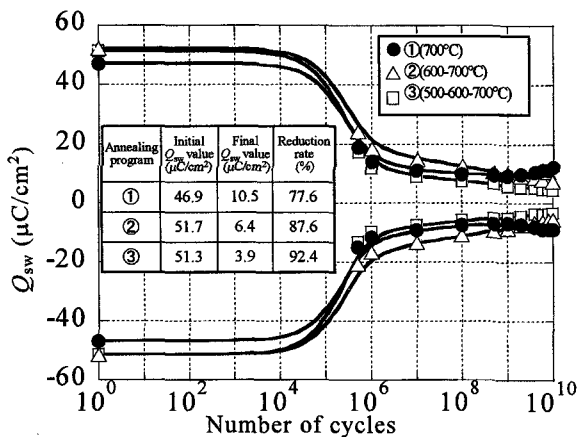


Fig. 5. Polarization fatigue characteristics of the three Pt/PZT/PbTiO<sub>3</sub>/Pt capacitors.

MgO(202), Pt(202) and PZT(101) is evidence of epitaxial growth. Epitaxial growth was observed in the PZT samples fabricated according to other two programs as well.

The *P-E* hysteresis loops of the three PZT samples crystallized by HIP are shown in Fig. 4. The PZT samples treated using all three annealing programs exhibited good symmetric hysteresis loop shapes with a remanent polarization of  $2P_r = 49\text{--}54 \mu\text{C}/\text{cm}^2$  and a coercive field of  $2E_c = 123\text{--}129 \text{ kV}/\text{cm}$ . Although the three PZT samples obtained yielded nearly equal performance, the PZT film crystallized using the multi-step annealing program 3 exhibited the best hysteresis loop shape with a relatively large remanent polarization of  $2P_r = 54 \mu\text{C}/\text{cm}^2$  and a coercive field of  $2E_c = 129 \text{ kV}/\text{cm}$ . On the other hand, the amplitudes of depolarization of the samples treated according to annealing programs 1, 2 and 3 were estimated to be  $10 \mu\text{C}/\text{cm}^2$ ,  $0.3 \mu\text{C}/\text{cm}^2$  and  $3.9 \mu\text{C}/\text{cm}^2$ , respectively, from the depolarization characteristics of the hysteresis loops. From the above results, it is clear that the single- and multi-step HIP-treatment annealing programs are very effective for completely crystallizing the amorphous PZT films.

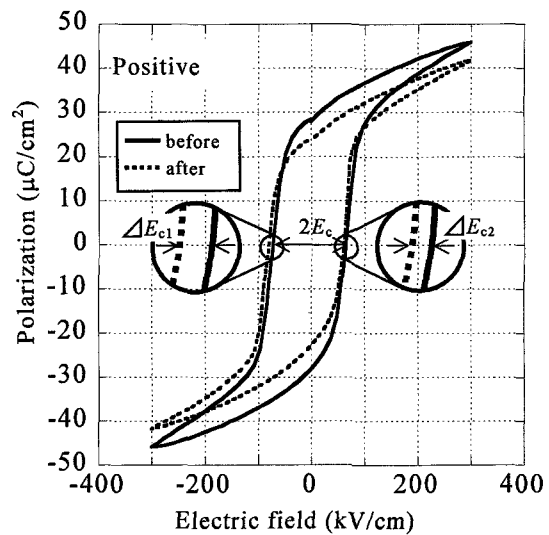


Fig. 6. Dynamic imprint characteristics of PZT film HIP-treated according to annealing program 3.

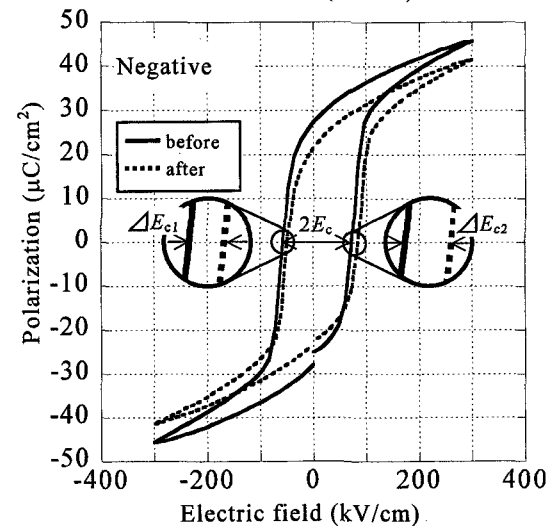


Fig. 6. Dynamic imprint characteristics of PZT film HIP-treated according to annealing program 3.

Figure 5 shows the polarization fatigue characteristics of the PZT films HIP-treated according to the three annealing programs. Measurements were conducted using an applied electric field of  $E = 2.5E_c$ . The appreciable fatigue degradation that was frequently observed through polarization fatigue tests in lead-based ferroelectric films<sup>8-10</sup>, was confirmed in the range of  $>1.0 \times 10^4$  switching cycles. The reduction rate of the pulse-derived switchable polarization,  $Q_{sw}$ , was calculated using the initial  $Q_{sw}$  value and final  $Q_{sw}$  value after  $1.0 \times 10^{10}$  cycles. These results are shown in the inset (table) in Fig. 5. It was shown from these results that although the initial  $Q_{sw}$  value of the PZT films HIP-treated at 1.5 MPa using a single-step ( $700^\circ\text{C}$ ) annealing program is slightly lower compared to those of the other PZT films, its polarization fatigue characteristics are relatively superior to them. This suggests that a longer retention time at a high temperature ( $700^\circ\text{C}$ ) is effective in completely crystallizing the PZT film from the amorphous state and stabilizing the  $\text{BO}_6$

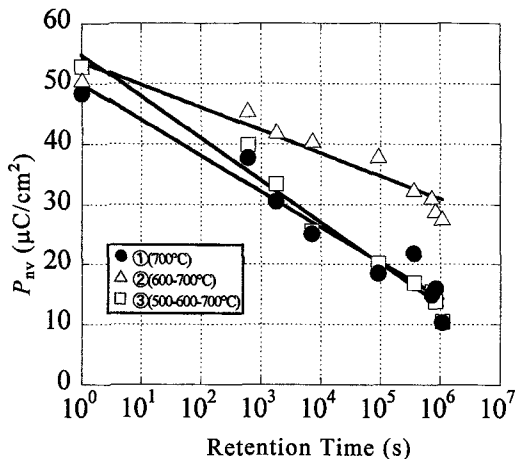


Fig. 7. Charge retention characteristics of PZT films at storing temperature of 150°C as a function of time, showing the charge in nonvolatile component,  $P_{nv}=P_s-P_{ns}$ , where  $P_s$  and  $P_{ns}$  are the switched and nonswitched polarizations, respectively.

octahedron of the perovskite structure.

Figure 6 shows the dynamic imprint characteristics of a typical PZT film HIP-treated according to annealing program 3 (500-600-700°C). The hysteresis loops for the positive and negative imprint tests after  $1.0 \times 10^{10}$  switching cycles shifted slightly to the negative and positive electric field directions, respectively. Here, the polarity is positive when a positive DC voltage is applied to the top Pt electrode. Similar shifts were observed as well as in the PZT samples fabricated according to the other two programs ranging from 4.7 to 6.1%. The shift  $s$  is defined as

$$s (\%) = \left\{ \frac{(\Delta E_{c1} + \Delta E_{c2})}{2} \right\} / 2E_c \times 100 \quad (2)$$

where  $s$  represents the rate of shift, and  $\Delta E_{c1}$  and  $\Delta E_{c2}$  represent the shift amounts of the negative and positive electric fields before and after the positive or negative imprint test, respectively. The charge retention characteristics of the three PZT samples at a storage temperature of 150°C as a function of time are shown in Fig. 7. For the three PZT samples, a significant decrease in polarization was observed at short times by preserving the samples at 150°C. Moreover, by comparing the three crystallization programs, it is apparent from the slope of the linear plots shown in Fig. 7 that the PZT film fabricated using program 2 exhibits the best retention characteristics. On the basis of the above results and the shape of hysteresis loops in Fig. 4, this retention behavior can be explained by the presumption that the retention characteristics can be improved as the depolarization becomes smaller, as previously observed in  $P$ - $E$  hysteresis loops. Based on the above results,  $\text{Pb}(\text{Zr}_{0.3}\text{Ti}_{0.7})\text{O}_3$  films crystallized by the two-step

(600-700°C) annealing program can be expected to be used as high-endurance and high-density FeRAM element materials.

#### 4. CONCLUSIONS

Epitaxial  $\text{Pb}(\text{Zr}_{0.3}\text{Ti}_{0.7})\text{O}_3$  films with uniform  $c$ -axis orientations were successfully fabricated on  $\text{PbTiO}_3/\text{Pt}(100)/\text{MgO}(100)$  substrates from an amorphous state by hot isostatic pressing (HIP). The results of this study can be summarized as follows.

1. The crystallized PZT films yielded a preferential (001) orientation with the degree of  $c$ -axis orientation of  $\alpha=0.68$ -0.72.
2. Based on the results of X-ray pole figures, all the PZT films fabricated using the three crystallization programs were almost completely epitaxial.
3. PZT film crystallized using the multi-step (500-600-700°C) annealing program 3 exhibited the best hysteresis loop shape with a relatively large remanent polarization of  $2P_r=54 \mu\text{C}/\text{cm}^2$  and a coercive field of  $2E_c=129 \text{ kV}/\text{cm}$ .
4. From measurements of fatigue, imprint and retention characteristics, PZT films HIP-treated at 1.5 MPa using a two-step (600-700°C) annealing program have the ability to be used as high-endurance and high-density element materials for FeRAM applications.

#### REFERENCES

- 1) M. T. Escote, F.M. Pontes, E. R. Leite and E. Long, *J. Appl. Phys.*, **96**, 2186 (2004).
- 2) M. Kobune, Y. Nishioka, T. Inoue and T. Yazawa, *J. Cryst. Growth*, in press.
- 3) A. Kakimi, S. Okamura and T. Tsukamoto, *Jpn. J. Appl. Phys.*, **33**, L1707 (1994).
- 4) A. Kakimi, S. Okamura, S. Ando and T. Tsukamoto, *Jpn. J. Appl. Phys.*, **34**, 5139 (1995).
- 5) M. Kobune, S. Kojima, Y. Nishioka, T. Yazawa, H. Fujisawa and M. Shimizu, *Integrated Ferroelectrics*, **63**, 105 (2004).
- 6) M. Kobune, S. Kojima, Y. Nishioka and T. Yazawa, *J. Jpn. Soc. Powder Powder Metallurgy*, **51**, 336 (2004).
- 7) H. Morioka, G. Asano, T. Oikawa and H. Funakubo, *Appl. Phys. Lett.*, **82**, 4761 (2003).
- 8) M. Kobune, O. Matsuura, T. Matsuzaki, A. Mineshige, S. Fuji, H. Fujisawa, M. Shimizu and H. Niu, *Jpn. J. Appl. Phys.*, **39**, 5451 (2000).
- 9) M. Kobune, O. Matsuura, T. Matsuzaki, T. Sawada, H. Fujisawa, M. Shimizu and H. Niu, *Ferroelectrics*, **271**, 199 (2002).
- 10) R. Wakabayashi, M. Kobune, T. Sawada, S. Kojima and K. Honda, *Integrated Ferroelectrics*, **46**, 27 (2002).